

Porous yttria-stabilized zirconia ceramics with ultra-low thermal conductivity. Part II: temperature dependence of thermophysical properties

Liangfa Hu · Chang-An Wang · Zijun Hu ·
Sheng Lu · Chencheng Sun · Yong Huang

Received: 20 April 2010 / Accepted: 20 July 2010 / Published online: 4 August 2010
© Springer Science+Business Media, LLC 2010

Abstract This study describes the experimental results of thermal diffusivity, specific heat at constant pressure, and thermal conductivity of porous 8 mol% yttria-stabilized zirconia (YSZ) ceramics in a temperature range from room temperature to 1,400 °C. It is a follow-up study of the earlier report titled by “Porous YSZ ceramics with ultra-low thermal conductivity”, which focused on the room-temperature thermal conductivity. The thermal diffusivity of porous YSZ ceramics decreased with the increase of the measurement temperature up to 600–1,000 °C, followed by an increasing trend with increasing temperature. The specific heat did not exhibit any significant dependence on sintering temperature and agreed with literature data. The thermal conductivity of the porous YSZ ceramics showed an insensitive tendency of change with measurement temperature. The thermal conductivity fell in groups by the sintering temperature level. This investigation also discussed an appropriate sintering temperature of porous YSZ ceramics, which had both low thermal conductivity and high strength required by the practical service.

Introduction

Many studies have focused on zirconia thermal barrier coatings (TBCs), which generally consist of yttria-stabilized zirconia with high thermal expansion coefficient, low thermal conductivity, and chemical inertness in combustion atmosphere [1–4], for applications in thermal insulations. These zirconia-based TBCs are widely used in gas turbine engines to protect the underlying metal from the high operating temperature and improve the durability of the components and engine efficiency [5–8]. The engineering performance of zirconia ceramics may be strongly affected by their responses to transient or steady-state heat transfer, each of which is governed by thermal diffusivity and thermal conductivity. For example, thermal conductivity is a critical design parameter of TBCs for aeronautic, astronautic, and land-based gas turbines. Therefore, to optimize their properties, it is important to have a reliable database and a satisfactory understanding of the physical process that is involved in heat transfer with the zirconia ceramics.

Some investigations have already been reported regarding the relationship between the thermal conductivity and the microstructure of zirconia-based TBCs [9–11]. The influence of the temperature and microstructure of single-layer coatings and multi-layer coatings on thermophysical properties at the same YSZ composition has also been reported [12]. Although TBCs offer advantage in thermal insulating, they provided little potential in load-bearing. TBCs cannot meet the strength requirement of thermal protections which require not only low thermal conductivity but also high strength. Therefore, it is important to study zirconia-based ceramics as bulk materials which meet both thermal and mechanical requirements. Furthermore, due to the high operating temperature, the temperature dependence of microstructure and

L. Hu · C.-A. Wang (✉) · Y. Huang
State Key Lab of New Ceramics and Fine Processing,
Department of Materials Science and Engineering, Tsinghua
University, Beijing 100084, People's Republic of China
e-mail: wangca@tsinghua.edu.cn

Z. Hu · S. Lu · C. Sun
National Key Lab of Advanced Functional Composite Materials,
Aerospace Research Institute of Materials & Processing
Technology, Beijing 100076, People's Republic of China

thermophysical properties of porous, bulk, zirconia ceramics is also an important consideration for thermal protections. This present study, for this reason, is focused on this point.

The earlier part of this study discussed the relationship between microstructure and room-temperature thermal conductivity of porous, bulk, 8 mol% yttria-stabilized zirconia (YSZ) ceramics. As a follow-up work, the present study involves measurements of the thermal diffusivity, specific heat at constant pressure of porous YSZ ceramics in a temperature range from room temperature to 1,400 °C, and thus calculations of the corresponding thermal conductivity. This study allows comparison of YSZ ceramics in a large range of yttria amount and porosity. To accomplish this, a series of porous YSZ ceramics with the same solid loading of 10 vol% were fabricated by varying the sintering temperature. A secondary ongoing objective of this investigation is to find an appropriate sintering temperature of porous YSZ ceramics, which have both low thermal conductivity and high strength required by the practical service.

Experimental procedure

Materials

Commercially available 8 mol% yttria-stabilized zirconia (YSZ) powder (AR grade, Shanghai Chemical Regent Co., China) was used as the starting material. This YSZ powder has an average particle size of 1.26 μm and a specific surface area of 6.49 m^2/g . Tert-butyl alcohol (TBA, chemical purity, Beijing Yili Chemical Co., Beijing, China) was used as shaping solvent and pore forming agent in gel-casting process. A premix solution of monomers and cross linker was prepared in TBA with a concentration of 14.5 wt% of acrylamide (AM, $\text{C}_2\text{H}_3\text{CONH}_2$) and 0.5 wt% *N,N'*-methylenebisacrylamide (MBAM, $(\text{C}_2\text{H}_3\text{CONH})_2\text{CH}_2$). Initiator and catalyst for gelation reaction are ammonium persulfate (APS) and *N,N,N,N*-tetramethylethylenediamine (TEMED), respectively. All chemicals used in this study are analytical grade.

Sample preparation

The TBA-based gel-casting technique typically consists of preparing a liquid suspension (slurry), molding, drying, binder removal, and sintering. Slurries with 10% solid loading, including YSZ powders, TBA, acrylamide (AM) were prepared by ball milling for 5 h. In order to adjust the suspension to a proper flowability during casting, selected alkali solution was added into the slurries. After ball milling, initiator and catalyst were mixed into the slurries. These slurries were poured into molds and dried at 52 °C in

nitrogen atmosphere. During the drying procedure, the polymerization of AM occurred and TBA gradually volatilized. Green bodies were then produced. Subsequently, they were sintered at different temperatures of 1400, 1450, 1500, and 1550 °C for 2 h.

Characterization

Thermal conductivity (λ) can be calculated from the thermal diffusivity (k), density (ρ), and specific heat at constant pressure (C_p):

$$\lambda = k \cdot \rho \cdot C_p \quad (1)$$

The thermal diffusivity (k) was measured at both ambient and elevated temperatures up to 1,400 °C using laser flash technique which was developed by Parker [13]. The detailed measurement technique was described elsewhere [14] and was briefly described here. This technique was employed on freestanding samples using a laser flash analyzer (LFA-427, Netzsch Instruments Inc., Germany). The freestanding samples were machined into 10 mm disks with height of 1 mm. Because of the translucency of the samples to the laser, the samples were sputter-coated a graphite layer (Aerodag G, Acheson Colloids Company, Port Huron, MI) in order to ensure complete and uniform absorption of the laser pulse prior to the thermal diffusivity measurement. The laser flash method involves heating one side of the sample with a laser pulse (duration: 0.6 ms; laser voltage: 410 V) and measuring the temperature rise on the rear surface with an infrared detector. The thermal diffusivity is determined from the time required to reach one-half of the peak temperature in the resulting temperature rise curve for the rear surface. All high temperature thermal diffusivity measurements were conducted in an argon atmosphere. Each value of thermal diffusivity represented the average value of three measurements. Some measurements were also performed during cooling to compare the difference between the respective heating and cooling values.

In order to determine the thermal diffusivity, the following temperature response on the rear surface of the sample is obtained:

$$\Delta T = \Delta T_m \left[1 + 2 \sum_{i=1}^{\infty} (-1)^i \exp\left(\frac{-n^2 \pi^2}{H^2} kt\right) \right] \quad (2)$$

where k and H are the thermal diffusivity and the thickness of the sample, respectively, ΔT is the temperature rise of the sample, ΔT_m its maximum value, and t the time after pulse heating. The thermal diffusivity is described by the following equation:

$$k = \frac{1.38H^2}{\pi^2 t_{1/2}} \quad (3)$$

where $t_{1/2}$ is the time period corresponding to a temperature rise to half of the maximum temperature on the rear surface of the sample.

The specific heat at constant pressure (C_p) was also measured in the same temperature range during heating using a differential scanning calorimeter (Netzsch STA 449F1) with reference materials of single-crystal alumina under air.

In polycrystalline isotropic materials, the density depends on temperature following the equation:

$$\rho(T) = \frac{\rho_{300}}{1 + 3\alpha\Delta T} \quad (4)$$

where $\rho(T)$ is the density at temperature T and ρ_{300} the density at 300 K, $\Delta T = T - 300$, and α the linear thermal expansion coefficient defined as:

$$\alpha = \frac{1}{L} \left(\frac{dL}{dT} \right)_p \quad (5)$$

where L is a characteristic length of the sample and T its temperature. The linear thermal expansion coefficient was measured using a DIL (402 PC, Netzsch Instruments Inc., Germany).

The porosity was calculated using mass and volume measurements to determine the density of the porous samples and then comparing this to the density of the fully dense ceramic, which was taken as 6.0 g/cm³ for this YSZ material. For the compressive strength measurements, samples with a diameter of 20 mm and a height of 20 mm were loaded with a crosshead speed of 0.05 mm/min

(CSS-2220 test machine). Three specimens with the same sintering conditions were used to determine the average porosity and compressive strength. The statistical uncertainty (error bar) was determined by calculating the standard deviation of the experimental data of the three specimens. Microstructure was observed using a scanning electron microscope (SEM, JSM 6700F, JEOL, Tokyo, Japan).

Results and discussions

Microstructure and porosity

Figure 1 shows the SEM micrographs of the porous YSZ ceramics sintered at different sintering temperatures of 1400, 1450, 1500, and 1550 °C. After the sintering processes, both TBA and PMA were successfully removed and porous YSZ bodies were obtained. The interconnected pores were homogeneously dispersed in the zirconia matrix. Adjacent grains interconnected to form a strong skeleton. It could be observed from Fig. 1a–d that the grains grew up and the porosity decreased as the sintering temperature increased from 1,400 to 1,550 °C.

Table 1 shows the variations of porosity and compressive strength of porous YSZ ceramics with sintering temperature. As the sintering temperature increased from 1,400 to 1,550 °C, the porosity decreased from 74 to 65% due to the process of sintering densification, while the compressive strength increased from 8 to 25 MPa.

Fig. 1 SEM micrographs of porous YSZ ceramics at different sintering temperatures: **a** 1400 °C, **b** 1450 °C, **c** 1500 °C, and **d** 1550 °C

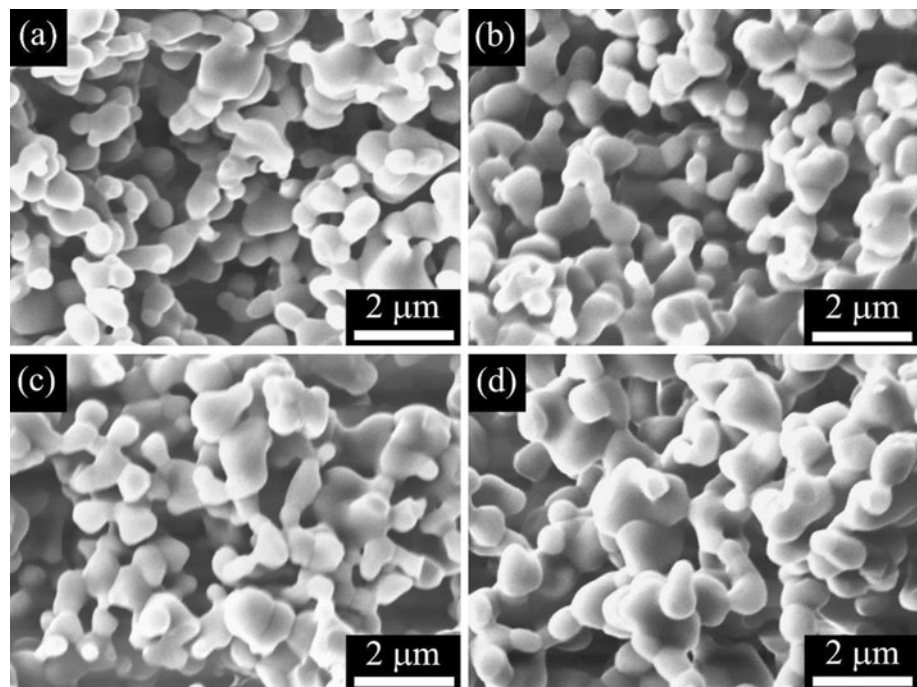
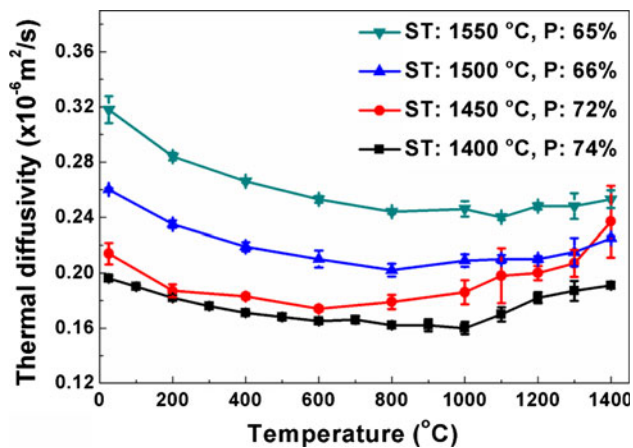


Table 1 Variations of porosity and compressive strength of porous YSZ ceramics with sintering temperature

Sample	Sintering temperature (°C)	Porosity (%)	Compressive strength (MPa)
A	1,400	74.2 ± 1.4	7.9 ± 0.5
B	1,450	72.0 ± 0.6	8.9 ± 0.5
C	1,500	66.0 ± 1.1	13.2 ± 0.5
D	1,550	65.1 ± 0.5	24.9 ± 2.4

**Fig. 2** Thermal diffusivity of porous YSZ ceramics with different sintering temperature and porosity as a function of the measurement temperature (*ST* sintering temperature, *P* porosity)

Thermophysical properties

Figure 2 shows the thermal diffusivity of the present samples with different sintering temperature and porosity as a function of the measurement temperature. It was observed that the thermal diffusivity of the samples decreased with the increase in temperature from low range of temperature up to 600–1,000 °C. As the temperature exceeded 1,000 °C, however, the thermal diffusivity increased slightly with increasing temperature. The downturn in the experimental curves in the low temperature range could be attributed to the increasing phonon-scattering with increasing temperature. In the higher temperature range, however, the thermal radiation became intense enough to influence significantly the thermal conduction. The reason for the slight increase of the thermal diffusivity with the increasing temperature (>1,000 °C) was the combination of thermal radiation and phonon scattering. Moreover, the thermal diffusivity fell in groups with the decrease of sintering temperature and with the increase of porosity. For example, the thermal diffusivity of the sample with sintering temperature of 1,550 °C and porosity of 65% was in the range between 0.32 and 0.25 ($\times 10^{-6}$ m²/s), but the corresponding value of the sample

with sintering temperature of 1,400 °C and porosity of 74% decreased to be 0.16–0.20 ($\times 10^{-6}$ m²/s). It was caused by the increasing porosity of porous YSZ ceramics, resulting in the enhancement of phonon scattering at pores. It was speculated [15] that the thermal diffusivity of yttria-stabilized zirconia of any density was not likely lower than 0.30 ($\times 10^{-6}$ m²/s), but the data for porous YSZ ceramics fabricated in the present study reached 0.16 ($\times 10^{-6}$ m²/s).

Table 2 lists the values for the specific heat for the porous YSZ ceramics with different sintering temperature, from room temperature to 1,400 °C. At a given measurement temperature, the variation of specific heat for samples with different sintering temperature was considerable. While the changing trends of the specific heat value with increasing measurement temperature were similar for the samples with different sintering temperature of 1400, 1450, 1500, and 1550 °C, respectively. The reasons for significant deviation of the specific heat at a given measurement temperature were not clear. The variation behavior of specific heat of YSZ ceramics on measurement temperature agreed with literature report [16].

The thermal conductivity of samples (open symbols) is plotted as a function of the measurement temperature with comparable data for bulk zirconia ceramics (closed symbols) from literatures [17–20] in Fig. 3. The thermal conductivity of the porous YSZ ceramics was insensitive to the change of measurement temperature. It was also shown that ZrO₂ fully stabilized with 12 mol% Y₂O₃ had a roughly constant thermal conductivity up to 1,200 °C [18]. However, the thermal conductivity of porous YSZ ceramics in the present study was much lower than the reported values of bulk YSZ ceramics with large range of yttria amounts and porosity from literatures [17–20]. The porosity of the porous YSZ ceramics was 65–74%, while the porosity of the YSZ ceramics in the cited literatures was 0 [17–19] or 37% [20]. Moreover, the thermal conductivity fell in groups by the sintering temperature level. For example, the thermal conductivity of the sample with sintering temperature of 1,550 °C was 0.29–0.34 W/m K, while the corresponding value of the sample with sintering temperature of 1,400 °C decreased to be 0.12–0.19 W/m K.

In the earlier studies of the heat conduction behavior of ZrO₂, Kingery et al. [21] and Mirkovitch [22] found that the thermal conductivity of polycrystalline ZrO₂ above room temperature was nearly independent of temperature. This temperature independence is the result of the high concentration of defects in the form of oxygen vacancies which limit the phonon mean-free-path to approximately the dimensions of the unit cell. This effect suppresses the $\approx 1/T$ dependence of the thermal conductivity on temperature which was claimed by Raghavan et al. [17] and proposed independently by Klemens [23] from theoretical considerations.

Table 2 Specific heat at constant pressure (J/kg K) of the porous YSZ ceramics with different sintering temperature, from room temperature to 1,400 °C

Sintering temperature (°C)	Measurement temperature (°C)										
	25	200	400	600	800	1,000	1,100	1,200	1,300	1,400	
1,400	491	552	533	524	505	489	624	693	555	653	
1,450	522	573	579	632	654	684	604	726	605	788	
1,500	491	577	624	693	710	716	715	747	643	760	
1,550	440	519	546	658	640	649	654	682	654	731	

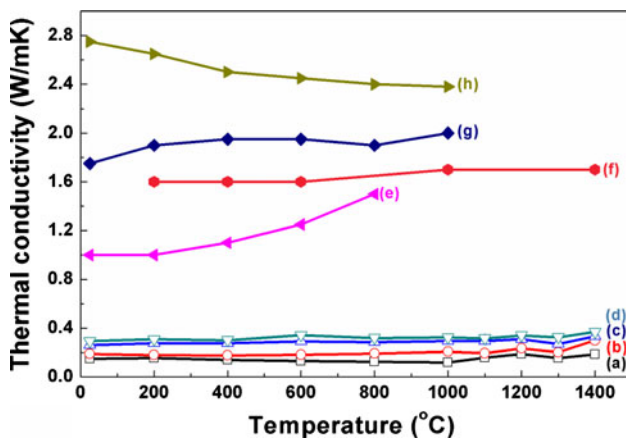


Fig. 3 Comparison of thermal conductivity for porous YSZ ceramics with different sintering temperatures ((a) 1400 °C, (b) 1450 °C, (c) 1500 °C, and (d) 1550 °C) of the present study (open symbols) with comparable data for bulk YSZ ceramics (closed symbols) from literatures: (e) porous 3 mol% YSZ with nano-sized grains and porosity of 37% [17], (f) dense 12 mol% YSZ [18], (g) dense 8 mol% YSZ [19], and (h) dense 4 mol% YSZ [20]

The presence of defects, such as pores, vacancies, pore-grain interfaces, and inclusions, contributes to the decrease of the thermal conductivity of a solid. Pores and interfaces primarily decrease the net section area through which heat is transported by phonon and so the reduction in thermal conductivity depends not only on the volume fraction but also on the architecture of pores. For example, Nicholls and his co-workers [24] reported that the porosity and/or defects provide a major contribution to the reduction of the thermal conductivity of plasma-sprayed coatings. It was also reported in the earlier part of this study that the room-temperature thermal conductivity for porous YSZ ceramics decreased with increasing porosity [25].

The higher porosity and the porous microstructure was believed to be the dominant factor for obtaining the lower thermal conductivity of the porous YSZ ceramics in the present study than that of bulk YSZ ceramics in previous literatures. The large amounts of interconnected pores made the ceramics grains not necessarily continuous or dispersed, blocking the heat conducting pathways and also contributing to the remarkably low level of thermal conductivity. Moreover, the large number of pores and

micro-sized interfaces provided significant phonon and photon scattering. In particular, the reason that the thermal conductivity fell in groups by the sintering temperature level was microstructural difference, such as higher porosity and looser connections between grains in the sample with lower sintering temperature than those of the sample with higher sintering temperature, as shown in Fig. 1.

As shown in Table 1 and Fig. 3, the thermal conductivity and compressive strength of the sample with sintering temperature of 1,550 °C were 0.29–0.34 W/m K and 25 MPa, respectively. This indicated that the sintering temperature of 1,550 °C was suitable for yielding porous YSZ ceramics which had both low thermal conductivity and high strength for applications in thermal insulators.

Conclusions

The thermal diffusivity of porous YSZ ceramics decreased and then increased, in a little range, with the increase of the measurement temperature. The specific heat did not show any significant dependence on sintering temperature or porosity and agreed with literature data. The thermal conductivity fell in groups by the sintering temperature level and was much lower than the reported values from literatures. This study also pointed out that the sintering temperature of 1,550 °C was suitable for yielding porous YSZ ceramics which had both low thermal conductivity and high strength for applications in thermal insulators.

Acknowledgement This study was supported by the National Natural Science Foundation of China (Grant No: 90816019), the Natural High Technology Research and Development Program of China (“863” Program, Grant No: 2007AA03Z435) and State Key Development Program of Basic Research of China (“973” program, Grant No: 2006CB605207-2).

References

1. Miller RA (1987) Surf Coat Technol 30:1
2. Wright PK (1999) Curr Opin Solid State Mater Sci 4:255
3. Stecura S (1977) Am Ceram Soc Bull 56:1082
4. Strangman TE (1985) Thin Solid Films 127:93

5. Padture NP, Gell M, Jordan EH (2000) *Science* 296:280
6. Miller RA (1999) *J Therm Spray Technol* 6:35
7. Wortman DJ, Nagaraj BA, Duderstadt EC (1989) *Mater Sci Eng A* 433:120
8. Zhu D, Miller RA (2000) *MRS Bull* 25:43
9. Schulz U, Fritscher K, Scheibe HJR, Kaysser WA, Peters M (1997) *Mater Sci Forum* 957:251
10. Peters M, Leyens C, Schulz U, Kaysser WA (2001) *Adv Eng Mater* 4:193
11. Nicholls JR (2003) *MRS Bull* 9:659
12. Jang BK (2009) *J Alloys Compd* 480:806
13. Parker WJ, Jenkins RJ, Abbott GL, Butler CP (1961) *J Appl Phys* 32(9):1679
14. ASTM Standard E 1461-01, Standard test method for thermal diffusivity of solids by the flash method, American Society for Testing and Materials, ASTM International, West Conshohocken, PA
15. Mirkovich VV (1976) *High Temp High Press* 8: 231
16. Touloukian YS, Buyco EH (1970) In: *Thermophysical properties of matter*, vol 5. Plenum, New York
17. Raghavan S, Wang H, Dinwiddie RB, Porter WD, Mayo MJ (1998) *Scr Mater* 39:1119
18. Eaton HE, Linsey JR, Dinwiddie RB (1994) In: Tong TW (ed) *Thermal conductivity*, vol 22. Technomic, Lancaster, PA
19. Schlichting KW, Padture NP, Klemens PG (2001) *J Mater Sci* 36:3003. doi:[10.1023/A:1017970924312](https://doi.org/10.1023/A:1017970924312)
20. Jang BK, Matsubara H (2006) *J Alloys Compd* 419:243
21. Kingery WD, Bowen HK, Uhlmann DR (1976) In: *Introduction to ceramics*, 2nd edn. Wiley, New York
22. Mirkovich VV (1965) *J Am Ceram Soc* 48(8):387
23. Klemens PG (1996) In: Wilkes KE, et al. (ed) *Thermal conductivity*, vol 23, pp 209–220. Technomic, Lancaster, PA
24. Nicholls JR, Lawson KJ, Johnstone A, Rickerby DS (2002) *Surf Coat Technol* 383:151
25. Hu L, Wang CA, Huang Y (2010) *J Mater Sci* 45:3242. doi:[10.1007/s10853-010-4331-9](https://doi.org/10.1007/s10853-010-4331-9)